RSC Advances

ROYAL SOCIETY OF CHEMISTRY

PAPER

View Article Online
View Journal | View Issue

Cite this: *RSC Adv.*, 2020, **10**, 9657

Synthesis and fluorescence properties of butadiyne-linked linear and cyclic carbazole oligomers†

Kazuya Ogawa,* Shohei Tanaka and Kyosuke Shimura

Received 28th January 2020
Accepted 27th February 2020

DOI: 10.1039/d0ra00830c

rsc.li/rsc-advances

Butadiyne-linked linear and cyclic carbazole oligomers were successfully synthesized. The intensity of the emission band in the 0–0 band of the highly planar macrocyclics decreased compared to that of the 0–1 band. Contrary to this, for larger macrocycles having reduced planarity, the intensity of the emission of the 0–0 band increased as in the cases of the linear compounds. This suggests that the emission color of the π-conjugated molecule can be controlled not only by the difference between the cyclic and chain structures but also by the control of the planarity, and is expected to be a new principle for molecular design in the development of fluorescent materials.

Introduction

The development of fluorescent molecules is attracting attention from the viewpoint of application to organic EL, bioimaging, two-photon fluorescent materials, and so on. In order to make a molecule that emits UV light emit visible light, it is necessary to expand the π-conjugation system to reduce the HOMO–LUMO energy difference, whereas the principle of molecular design for controlling the emission colour is required. Carbazole has a planar structure in which two benzene rings are bridged by a nitrogen atom, and exhibit strong UV emission. Several carbazole oligomers and polymers have been reported so far.[1–11] Since the bond angle between the 3- and 6-positions of carbazole is 90°, the oligomerization from these positions is expected to construct a stable cyclic tetramer. So, ethynyl-linked[1,6,8] and directly linked[5,11] cyclic carbazole tetramers have been synthesized. However, there have been no reports on butadiyne-linked cyclic tetramer or short oligomers connected at the 3,6-positions except for trimers and tetramers linked at the 1,8-positions.[9] It has been reported that two-photon absorption efficiency can be greatly improved by using the butadiyne linkage to connect π-conjugated systems between porphyrins.[12,13] Further, macrocyclic compounds composed of self-assembled porphyrins linked with fluorene[14] or carbazole[15] using the ethynylene linkage resulted in two-photon absorption enhancement. In this study, we report synthesis of butadiyne-linked linear and cyclic carbazole oligomers connected at the 3,6-positions, and their absorption and photoluminescence properties. In addition, attention has recently been focused on the emission properties of π-conjugated cyclic compounds,[16–31] and this study may also be interesting in this respect. The structures of synthesized compounds monomer **1**, linear trimer **3L**, linear tetramer **4L**, cyclic trimer **3R**, cyclic tetramer **4R**, cyclic pentamer **5R**, and cyclic hexamer **6R** are presented in Scheme 1.

Results and discussion

Synthesis

All the butadiyne-linked oligomers were synthesized using $Pd(PPh_3)_2Cl_2$ under an oxygen atmosphere in THF/triethylamine.[32] **3R**, **4R**, and **5R** were prepared at 60 °C for 26 hours. In the analytical GPC (gel permeation chromatography) data using chroloform as an eluent after the reaction (ESI†), main three peaks corresponding to **3R** and **5R** as well as **4R** were observed. Each peak was isolated using preparative GPC with the yields of 6% for **3R**, 11% for **4R**, and 6% for **5R**, respectively. In order to suppress cyclization, synthesis of **3L** and **4L** was performed by reducing the amount of $Pd(PPh_3)_2Cl_2$ and lowering the reaction temperature to 50 °C as compared to the synthesis of the cyclic compounds. Each compound was isolated using preparative GPC with the yields of 2% for **3L** and 4% for **4L**, respectively. In ^{1}H NMR spectra of **3L** and **4L**, a signal of the terminal alkyne, which disappeared in the cyclic compounds **3R** and **4R**, was observed at 3.09–3.10 ppm as two protons (ESI†). Further, in the MALDI-TOF MASS measurements, the molecular ion peaks of **3L** and **4L** were two hydrogens larger than those of the corresponding cyclic molecules **3R** and **4R** (ESI†). The cyclic hexamer **6R** could be synthesized from linear trimer **3L** with the formation of **3R**, and separated by preparative GPC with 20% yield. Fig. 1 and 2 show the analytical GPC chart containing all isolated compounds and logarithm plots of molecular weight *vs.* retention time, respectively. As seen in Fig. 2, **6R** fits on the GPC calibration curve drawn from **3R**, **4R**, and **5R** instead of **3L** and

Graduate Faculty of Interdisciplinary Research, University of Yamanashi, 4-3-11 Takeda, Kofu, Yamanashi 400-8511, Japan. E-mail: kogawa@yamanashi.ac.jp

† Electronic supplementary information (ESI) available: Data for GPC, NMR, mass, and quantum chemical calculations. See DOI: 10.1039/d0ra00830c

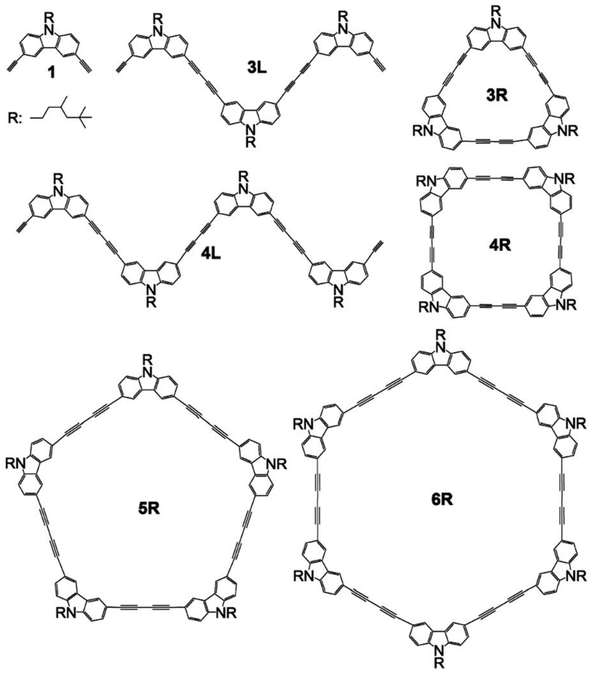

Scheme 1 Structures of **1**, **3L**, **4L**, **3R**, **4R**, **5R**, and **6R**.

4L. In the NMR spectra of **6R**, the terminal alkyne signal was not observed, and one set of carbazole was observed as seen in **3R** and **4R**. These data indicate the formation of **6R**.

Optical properties

The absorption and fluorescence spectra of synthesized compounds were measured in chloroform at room temperature. Comparing the linear compounds **3L** and **4L**, both the absorption and fluorescence of **4L** shifted slightly longer than those of **3L** due to the expansion of the π-conjugation, and the shapes of the spectra were similar (Fig. 3). **3L** and **4L** showed light blue emission as shown in Fig. 4.

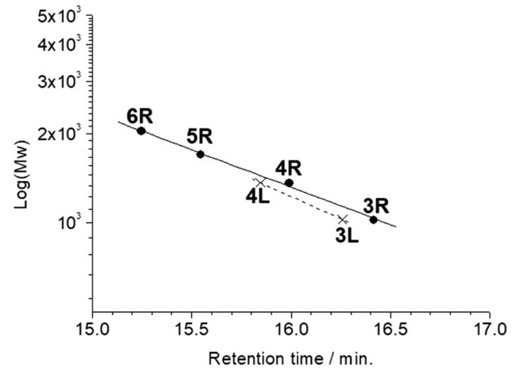

Fig. 2 Logarithm plots of molecular weight *vs.* retention time.

Secondly, cyclic compounds **3R** and **4R** were examined (Fig. 5). Compared with **3L** and **4L**, the absorption intensity around at 370 to 390 nm became weak, and these split into two peaks probably due to changes in vibration mode, but not clearly at this time. In the fluorescence spectra, emission from the 0–0 band near 400 nm was also weak. These results indicate that the cyclization changed the spectral shape for trimer and tetramer. The fluorescence spectra did not depend on concentration and solvent (acetone, THF, toluene, and hexane). A similar result was reported for cyclic and linear thiophene oligomers, where the intensity of the 0–0 band of the highly planar cyclic compound was lower than that of the linear structure.[26] **3R** and **4R** emitted blue light as presented in Fig. 4 due to the shift of the maximum emission band to around 440 nm.

Next, the larger macrocycles **5R** and **6R** were measured. As shown in Fig. 6, although these are cyclic molecules, the shapes of the fluorescence spectra are different from those of **3R** and **4R**. The emission intensity from the 0–0 band around 400 nm increased similar to the linear molecules **3L** and **4L**, and a band around 500 nm, which was observed as small shoulder in other compounds, appeared clearly. In the absorption spectra, the absorption intensities at 380 to 390 nm were intermediate

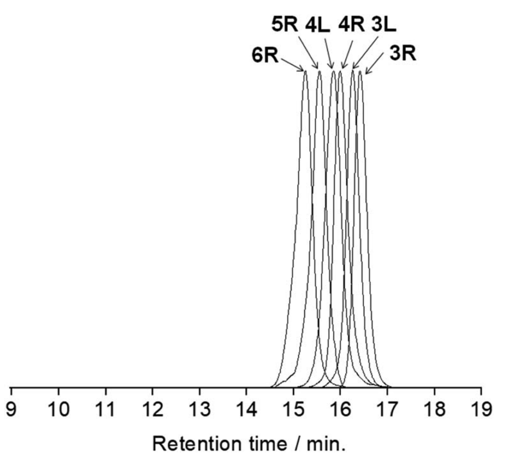

Fig. 1 The analytical GPC chart containing all isolated compounds. Chroloform was used as an eluent.

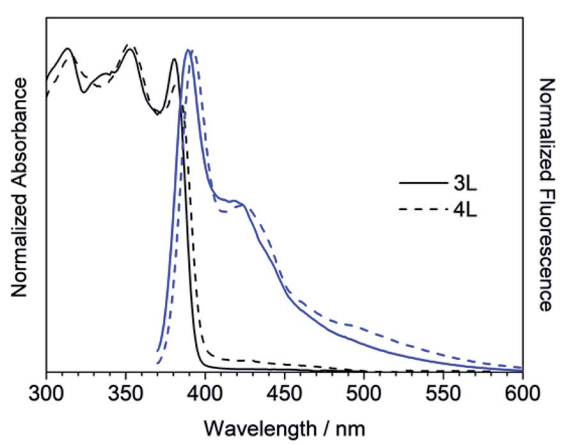

Fig. 3 UV/Vis absorption (black) and fluorescence (blue) spectra of **3L** and **4L** in chloroform.

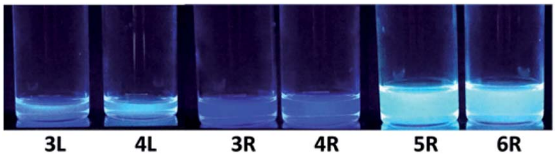

Fig. 4 Emission colour excited at 365 nm.

between linear and cyclic compounds for trimers and tetramers, and the splitting disappeared like linear molecules. These data indicate that the increase in the ring size increased the flexibility and lowered the planarity. These results are also consistent with the reversal of the relationship between the 0–0 and 0–1 band intensities obtained for the larger cyclic oligothiophene.[26] For the emission band around 500 nm, although clear information cannot be obtained from the absorption spectra, it may be a change in the vibration mode due to the increase in carbazole unit and flexibility. In the case of the ethynylene-linked cyclic tetramer in THF solution,[6] the S_0–S_1 absorption around at 375 nm was relatively weak, whereas the maximum fluorescence probably emitted from 0–0 band was observed at around 410 nm contrary to this study. On the other hand, the directly linked cyclic oligomer (mixture of 4-mer to 12-mer) exhibited higher emission intensity from the 0–1 band than the 0–0 band.[5] The butadiyne-linked carbazole tetramer connected at the 1,8-positions also showed stronger emission in the 0–1 band, but in trimer, the 0–0 band was stronger.[9] As seen in Fig. 4, the emission colour of **5R** and **6R** became light blue near white due to the relatively strong emission at around 500 nm.

Absorption and fluorescence data are summarized in Table 1. Increasing the number of units to 5 and 6 reduced the quantum yield. In **4R**, since the bond angle is 90° between carbazole 3- and 6-positions, the steric distortion is the smallest among the cyclic compounds giving the relatively large quantum yield value.

Quantum chemical calculations using Gaussian 09 were performed to further investigate these absorption and fluorescence properties. Geometry optimization in the ground state

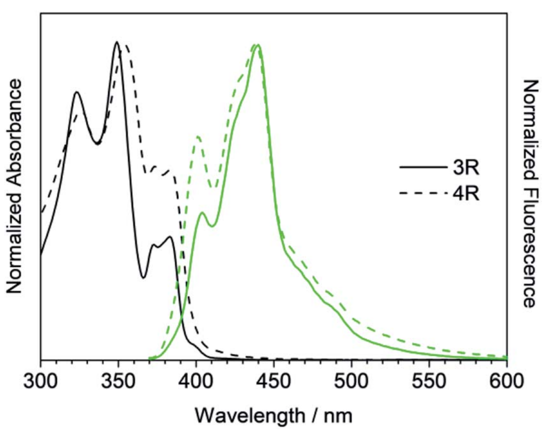

Fig. 5 UV/Vis absorption (black) and fluorescence (green) spectra of 3R and 4R.

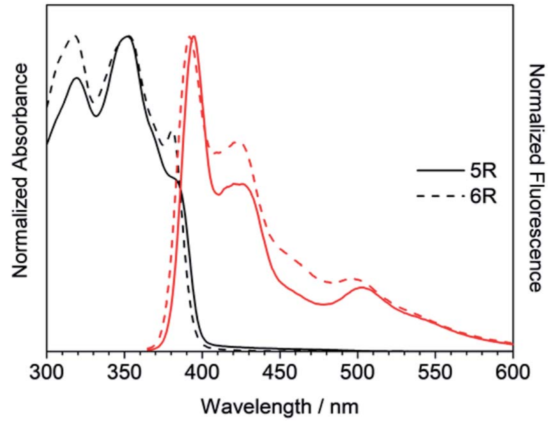

Fig. 6 UV/Vis absorption (black) and fluorescence (red) spectra of 5R and 6R.

was calculated using DFT with CAM-B3LYP and 6-31G(d). Chloroform was used as a solvent, and CPCM was employed as a solvent model. To increase the calculation speed, the trimethylhexyl group at the N-position was converted to a methyl group. Fig. S16 and S17 in ESI† show the optimized structures of **3L** and **4L**. Since **3L** and **4L** have a chain structure, the rotation barrier of the triple bond is relatively low, so that they are flexible and do not have rigid planarity. In the solution, various conformations other than the optimized structure may be taken due to the flexibility. On the other hand, **3R** and **4R** have complete planar structures, as demonstrated in Fig. 7 and 8. However, even in the cyclic structure, the planar geometry cannot be maintained in **5R** and **6R** due to increased flexibility (ESI†). Again, for **5R** and **6R**, various conformations other than optimized structures can be adopted in solution. According to the theory,[25] the ratio of 0–0 and 0–1 bands responds to the product of the exciton coherence number and the conformation factor, where the model shows that the 0–0 band is highly sensitive to chain bending. This may explain the small 0–0 bands observed in **3R** and **4R** without chain bending.

Next, in order to investigate the effect of the molecular structure on the electronic transition, the excited state was calculated by TD-DFT. The S_0–S_1 transitions for **3R** and **4R** were calculated as forbidden with the oscillator strength of zero due to the cancellation of the transition dipole (ESI†). In contrast, the S_0–S_1 transitions in the chain origomers **3L** and **4L**, and

Table 1 Photophysical data of carbazole oligomers

Compound	Absorption/nm	Fluorescence[a]/nm	Quantum yield
3L	381	389, 419	0.08
3R	373, 383	404, 440	0.08
4L	382	392, 423	0.17
4R	373, 383	401, 438	0.18
5R	380–385 (shoulder)	394, 429, 503	0.15
6R	381	392, 424, 497	0.11

[a] The excitation wavelengths for fluorescence measurements were selected to the absorption peak around 350 nm.

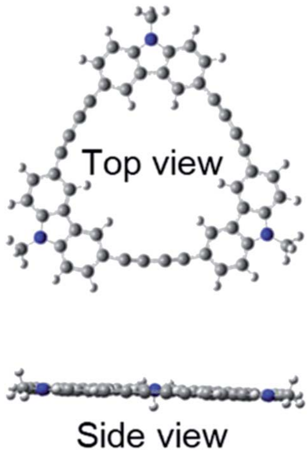

Fig. 7 Optimized structure of 3R.

large rings **5R** and **6R** were allowed because flexibility and low planarity eliminate the transition dipole cancellation. These results correspond to the fact that the absorption bands at around 380 nm for **3R** and **4R** were weaker than other oligomers. Further, the HOMO–LUMO absorption intensity of **3R** was about half compared to that of **4R**, suggesting that **4R** was more flexible than **3R** due to increased number of carbazoles and triple bonds. From the results at the calculation level used in this study, further quantitative discussion seems to be difficult between experimental and calculated values for wavelength and oscillator strength. For comparison, the calculated oscillator strengths were plotted *vs.* wavelength together with measured spectra (ESI†). Still, the question remains that the fluorescence quantum yields of **3R** and **4R** are not lower compared with **3L** and **4L**. Further, from the experimental results including ^{1}H NMR, where no significant ring current effect was observed in **3R** and **4R**, it cannot be judged whether the cyclic conjugate is stronger than linear. More detailed theoretical calculations including vibrations, and time-resolved measurements will be needed to clear these.

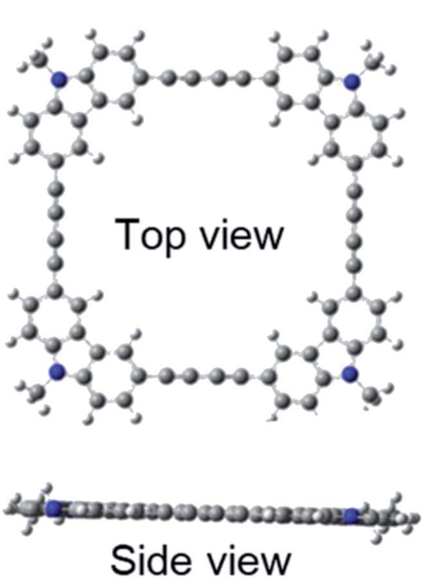

Fig. 8 Optimized structure of 4R.

Experimental

General procedures

Analytical GPC measurements were performed using an Agilent 1100 HPLC system with a JAIGEL 3HA column. Preparative GPC separations were made using a JAI LC-908 recycling HPLC system with two JAIGEL 3H columns in series. ^{1}H NMR spectra were recorded on Bruker AV III 500 HD spectrometer. UV-vis spectra were measured using a JASCO V-630 spectrometer. Fluorescence measurements were performed on a Hitachi F-2500 spectrophotometer. MALDI-TOF mass spectra were obtained with a Bruker Autoflex with dithranol as a matrix. 3,6-Diiodo-9-(3,5,5-trimethyl)hexylcarbazole was prepared according to the literature.[15]

3,6-Bis(trimethylsilylethynyl)-9-(3,5,5-trimethyl)hexylcarbazole. Under a nitrogen atmosphere, after dissolving 3,6-diiodo-9-(3,5,5-trimethyl)hexylcarbazole (0.25 g, 0.46 mmol), $Pd(PPh_3)_2Cl_2$ (0.1 g, 0.17 mmol), CuI (0.01 g, 0.34 mmol), and triethylamine (15 ml) in dry THF (75 ml), TMS-acetylene (0.2 ml, 1.42 mmol) was added to the solution and stirred at 40 °C for 6.5 hours. Saturated aqueous ammonium chloride solution was added, and the mixture was extracted with chloroform. Purification by silica gel column chromatography (hexane : chloroform = 3 : 1) gave a viscous yellow liquid to yield 0.21 g (0.43 mmol, 91%). ^{1}H NMR (500 MHz, $CDCl_3$): δ = 8.19 (d, 2H), 7.56–7.58 (dd, 2H), 7.26–7.28 (d, 2H), 4.22–4.29 (m, 2H), 1.76–1.84 (m, 1H), 1.59–1.65 (m, 2H), 1.14–1.30 (dd, 3H), 1.07–1.08 (d, 2H), 0.87 (s, 9H), 0.30 (s, 18H) ppm.

3,6-Diethynyl-9-(3,5,5-trimethyl)hexylcarbazole 1. After dissolving 3,6-bis(trimethylsilylethynyl)-9-(3,5,5-trimethyl)hexylcarbazole (0.21 g, 0.44 mol) in $CHCl_3$ (100 ml), TBAF (0.4 ml, 1.14 mmol) was added, and the mixture was stirred at room temperature for 3 hours. Silica gel column chromatography was performed to give **1** in 87% yield. ^{1}H NMR (500 MHz, $CDCl_3$): δ = 8.21 (d, 2H), 7.59–7.61 (dd, 2H), 7.30–7.32 (d, 2H), 4.22–4.29 (m, 2H), 3.08 (s, 2H), 1.79–1.87 (m, 1H), 1.59–1.67 (m, 2H), 1.15–1.31 (dd, 3H), 1.08–1.09 (d, 2H), 0.87 (s, 9H) ppm.

3R, 4R, and 5R.[32] Under an oxygen atmosphere, **1** (70 mg, 0.20 mmol), $Pd(PPh_3)_2Cl_2$ (140 mg, 0.16 mmol), and triethylamine (15 ml) were dissolved in dry THF (70 ml), and the mixture was stirred at 60 °C. After stirring for 23 h, water was added and extracted with chloroform. The solution was washed with saturated aqueous NH_4Cl and water. The crude was purified by preparative GPC (column; JAIGEL 3H, eluent; chloroform) to give **3R** (6%), **4R** (11%), and **5R** (6%). **3R:** ^{1}H NMR (500 MHz, $CDCl_3$): δ = 8.44 (d, 6H), 7.56–7.58 (dd, 6H), 7.32–7.34 (d, 6H), 4.24–4.32 (m, 6H),1.83–1.90 (m, 3H), 1.63–1.71 (m, 6H), 1.17–1.32 (s, 9H), 1.11–1.12 (d, 6H), 0.89 (s, 27H) ppm; MALDI-TOF Mass calcd for $C_{75}H_{75}N_3$: 1017.60, found: 1018.01 $[M + H]^+$; UV/Vis ($CHCl_3$) λ_{max}/nm (ε/mol^{-1} dm^3 cm^{-1}) = 323 (76 600), 349 (90 800), 373 (33 000), 383 (35 300). **4R:** ^{1}H NMR (500 MHz, $CDCl_3$): δ = 8.33 (d, 8H), 7.66–7.68 (dd, 8H), 7.34–7.36 (d, 8H), 4.24–4.32 (m, 8H), 1.82–1.89 (m, 4H), 1.63–1.67 (m, 8H), 1.18–1.33 (m, 12H), 1.11–1.12 (d, 8H), 0.89 (s, 36H) ppm; MALDI-TOF

Mass calcd for $C_{100}H_{100}N_4$: 1356.79; found: 1357.33 $[M + H]^+$; UV/Vis ($CHCl_3$) λ_{max}/nm (ε/mol^{-1} dm^3 cm^{-1}) = 326 (75 200), 354 (95 000), 373 (58 300), 383 (57 300). **5R:** ^{1}H NMR (500 MHz, $CDCl_3$): δ = 8.28 (d, 10H), 7.68–7.70 (dd, 10H), 7.34–7.36 (d, 10H), 4.24–4.33 (m, 10H), 1.83–1.88 (m, 5H), 1.63–1.70 (m, 10H), 1.17–1.33 (m, 15H), 1.11–1.12 (d, 10H), 0.89 (s, 45H) ppm; MALDI-TOF Mass calcd for $C_{125}H_{125}N_5$: 1695.99; found: 1696.71 $[M + H]^+$; UV/Vis ($CHCl_3$) λ_{max}/nm (ε/mol^{-1} dm^3 cm^{-1}) = 319 (86 900), 352 (100 000), 380 (55 500).

3L and 4L. Under an oxygen atmosphere, **1** (100 mg, 0.29 mmol), $Pd(PPh_3)_2Cl_2$ (100 mg, 0.11 mmol), and triethylamine (20 ml) were dissolved in dry THF (70 ml), and the mixture was stirred at 50 °C. After stirring for 53 h, water was added and extracted with chloroform. The solution was washed with saturated aqueous NH_4Cl and water. The crude was purified by preparative GPC (column; JAIGEL 3H, eluent; chloroform) to give **3L** (2%) and **4L** (4%). **3L:** ^{1}H NMR (500 MHz, $CDCl_3$): δ = 8.28–8.29 (dd, 4H), 8.24 (d, 2H), 7.66–7.69 (m, 4H), 7.61–7.63 (dd, 2H), 7.32–7.36 (m, 6H), 4.25–4.33 (m, 6H), 3.09 (s, 2H), 1.81–1.89 (m, 3H), 1.63–1.69 (m, 6H), 1.16–1.32 (m, 9H), 1.11–1.12 (d, 6H), 0.88 (s, 27H) ppm; MALDI-TOF Mass calcd for $C_{75}H_{77}N_3$: 1019.61; found: 1020.03 $[M + H]^+$; UV/Vis ($CHCl_3$) λ_{max}/nm (ε/mol^{-1} dm^3 cm^{-1}) = 313 (70 300), 353 (70 200), 381 (68 000). **4L:** ^{1}H NMR (500 MHz, $CDCl_3$): δ = 8.24–8.33 (m, 8H), 7.61–7.70 (m, 8H), 7.32–7.36 (m, 8H), 4.24–4.32 (m, 8H), 3.10 (s, 2H), 1.82–1.89 (m, 4H), 1.63–1.67 (m, 8H), 1.16–1.33 (m, 12H), 1.10–1.12 (m, 8H), 0.89 (s, 36H) ppm; MALDI-TOF Mass calcd for $C_{100}H_{102}N_4$: 1358.81; found: 1359.34 $[M + H]^+$; UV/Vis ($CHCl_3$) λ_{max}/nm (ε/mol^{-1} dm^3 cm^{-1}) = 315 (78 600), 353 (81 600), 382 (71 600).

6R. Under an oxygen atmosphere, **3R** (8 mg, 7.63 μmol), $Pd(PPh_3)_2Cl_2$ (8 mg, 8.8 μmol), and triethylamine (2 ml) were dissolved in dry THF (10 ml), and the mixture was stirred at 60 °C. After stirring for 21 h, water was added and extracted with chloroform. The solution was washed with saturated aqueous NH_4Cl and water. The crude was purified by preparative GPC (column; JAIGEL 3H, eluent; chloroform) to give **6R** (20%). ^{1}H NMR (500 MHz, $CDCl_3$): δ = 8.29 (d, 12H), 7.65–7.67 (dd, 12H), 7.33–7.35 (d, 12H), 4.22–4.32 (m, 12H), 1.81–1.89 (m, 6H), 1.62–1.70 (m, 12H), 1.16–1.32 (m, 18H), 1.10–1.11 (d, 12H), 0.88 (s, 54H) ppm; MALDI-TOF Mass calcd for $C_{150}H_{150}N_6$: 2035.19; found: 2036.29 $[M + H]^+$; UV/Vis ($CHCl_3$) λ_{max}/nm (ε/mol^{-1} dm^3 cm^{-1}) = 317 (90 400), 353 (90 100), 381 (63 200).

Summary

In summary, we succeeded in synthesizing butadiyne-linked linear and cyclic carbazole oligomers. Although the cyclic tetramer **4R** having a stable structure was expected to be the main product, **3L**, **4L**, **3R**, and **5R** could also successfully be isolated. Furthermore, a cyclic hexamer **6R** could be synthesized from **3L**. As pointed out in the literatures,[25,26] the intensity of the emission band in the 0–0 band of the highly planar macrocyclics **3R** and **4R** decreased compared to that of the 0–1 band. On the other hand, in the macrocycles **5R** and **6R** having reduced planarity, the intensity of the emission band of the 0–0 band increased as in the cases of the linear compounds **3L** and **4L**. As a result, by controlling the oligomer structure, different emission colors, light blue (**3L** and **4L**), blue (**3R** and **4R**), and pale blue close to white (**5R** and **6R**) could be expressed. This indicates that the emission color of the π-conjugated molecule can be controlled not only by the difference between the cyclic and chain structures but also by the control of the planarity, and is expected to be a new principle for molecular design in the development of fluorescent materials. Further, these compounds will be evaluated as two-photon fluorescent materials expected to be applied to 3D displays and other applications.

Conflicts of interest

There are no conflicts to declare.

Acknowledgements

This work was supported by Grant-in-Aids for Scientific Research (C) (no. 18K05258) from Ministry of Education, Culture, Sports, Science and Technology, Japan (Monbu Kagakusho). The MALDI-TOF measurement was carried out at Instrumental Analysis Center at Yokohama National University.

Notes and references

1 W. Zhang and J. S. Moore, *J. Am. Chem. Soc.*, 2004, **126**, 12796.
2 Y. Zhang, T. Wada and H. Sasabe, *J. Polym. Sci., Part A: Polym. Chem.*, 1997, **35**, 2041–2047.
3 S. Maruyama, Y. Zhang, T. Wada and H. Sasabe, *J. Chem. Soc., Perkin Trans. 1*, 1999, 41–46, DOI: 10.1039/A807158F.
4 S. Maruyama, H. Suzuki, X.-t. Tao, T. Wada, H. Sasabe, S. Miyata and T. Kamata, *Phys. Chem. Chem. Phys.*, 2000, **2**, 3565–3569.
5 J. Ostrauskaite and P. Strohriegl, *Macromol. Chem. Phys.*, 2003, **204**, 1713–1718.
6 K. Balakrishnan, A. Datar, W. Zhang, X. Yang, T. Naddo, J. Huang, J. Zuo, M. Yen, J. S. Moore and L. Zang, *J. Am. Chem. Soc.*, 2006, **128**, 6576–6577.
7 B. Schmaltz, A. Rouhanipour, H. J. Räder, W. Pisula and K. Müllen, *Angew. Chem., Int. Ed.*, 2009, **48**, 720–724.
8 A. D. Finke, D. E. Gross, A. Han and J. S. Moore, *J. Am. Chem. Soc.*, 2011, **133**, 14063–14070.
9 C. Maeda, T. Yoneda, N. Aratani, M.-C. Yoon, J. M. Lim, D. Kim, N. Yoshioka and A. Osuka, *Angew. Chem., Int. Ed.*, 2011, **50**, 5691–5694.
10 Z. J. Wang, S. Ghasimi, K. Landfester and K. A. Zhang, *Chem. Commun.*, 2014, **50**, 8177–8180.
11 L. S. Coumont and J. G. C. Veinot, *Tetrahedron Lett.*, 2015, **56**, 5595–5598.
12 K. Ogawa, A. Ohashi, Y. Kobuke, K. Kamada and K. Ohta, *J. Am. Chem. Soc.*, 2003, **125**, 13356–13357.
13 M. Drobizhev, Y. Stepanenko, Y. Dzenis, A. Karotki, A. Rebane, P. N. Taylor and H. L. Anderson, *J. Am. Chem. Soc.*, 2004, **126**, 15352–15353.

14 J. E. Raymond, A. Bhaskar, T. Goodson, N. Makiuchi, K. Ogawa and Y. Kobuke, *J. Am. Chem. Soc.*, 2008, **130**, 17212–17213.
15 O. Varnavski, J. E. Raymond, Z. S. Yoon, T. Yotsutuji, K. Ogawa, Y. Kobuke and T. Goodson, *J. Phys. Chem. C*, 2014, **118**, 28474–28481.
16 J. Kromer, I. I. Rios-Carreras, G. Fuhrmann, C. Musch, M. Wunderlin, T. Debaerdemaeker, E. Mena-Osteritz and P. Bauerle, *Angew. Chem., Int. Ed. Engl.*, 2000, **39**, 3481–3486.
17 M. Mayor and C. Didschies, *Angew. Chem., Int. Ed. Engl.*, 2003, **42**, 3176–3179.
18 B. M. Wong, *J. Phys. Chem. C*, 2009, **113**, 21921–21927.
19 F. Zhang, G. Gotz, H. D. Winkler, C. A. Schalley and P. Bauerle, *Angew. Chem., Int. Ed. Engl.*, 2009, **48**, 6632–6635.
20 S. Yamago, Y. Watanabe and T. Iwamoto, *Angew. Chem., Int. Ed.*, 2010, **49**, 757–759.
21 J. E. Donehue, O. P. Varnavski, R. Cemborski, M. Iyoda and T. Goodson, *J. Am. Chem. Soc.*, 2011, **133**, 4819–4828.
22 T. Iwamoto, Y. Watanabe, Y. Sakamoto, T. Suzuki and S. Yamago, *J. Am. Chem. Soc.*, 2011, **133**, 8354–8361.
23 T. J. Sisto, M. R. Golder, E. S. Hirst and R. Jasti, *J. Am. Chem. Soc.*, 2011, **133**, 15800–15802.
24 T. Nishihara, Y. Segawa, K. Itami and Y. Kanemitsu, *J. Phys. Chem. Lett.*, 2012, **3**, 3125–3128.
25 N. J. Hestand and F. C. Spano, *J. Phys. Chem. B*, 2014, **118**, 8352–8363.
26 P. Kim, K. H. Park, W. Kim, T. Tamachi, M. Iyoda and D. Kim, *J. Phys. Chem. Lett.*, 2015, **6**, 451–456.
27 C.-K. Yong, P. Parkinson, D. V. Kondratuk, W.-H. Chen, A. Stannard, A. Summerfield, J. K. Sprafke, M. C. O'Sullivan, P. H. Beton, H. L. Anderson and L. M. Herz, *Chem. Sci.*, 2015, **6**, 181–189.
28 F. Chen, Y. S. Hong, S. Shimizu, D. Kim, T. Tanaka and A. Osuka, *Angew. Chem., Int. Ed.*, 2015, **54**, 10639–10642.
29 Y. Nagata, S. Kato, Y. Miyake and H. Shinokubo, *Org. Lett.*, 2017, **19**, 2718–2721.
30 F. Chen, T. Tanaka, T. Mori and A. Osuka, *Chem.–Eur. J.*, 2018, **24**, 7489–7497.
31 Y. Matsuo, F. Chen, K. Kise, T. Tanaka and A. Osuka, *Chem. Sci.*, 2019, **10**, 11006–11012.
32 R. W. Wagner, T. E. Johnson, F. Li and J. S. Lindsey, *J. Org. Chem.*, 1995, **60**, 5266–5273.

